Electronic Supplementary Information (ESI)

Balancing Fluorine Density and Pore Architecture in Nanoporous Polyketaminal Networks for Exceptional SF_6/N_2 Separation

Qilin Wang,[a†] Hanrui Zhang,[a†] Jiangli Zhu,[a] Jun Yan,*[a,b] Zefeng Wang*[c,d] and Shengwei Guo *[a,b]

[a]*School of Materials Science and Engineering, North Minzu University, Yinchuan 750021, China*

[b]*Institute of Functional and Structural Characteristic Materials, Helanshan Laboratory Yinchuan 750021, China*

[c]*College of Ecology, Lishui University, Lishui 323000, China*

[d]*R&D Center of Green Manufacturing New Materials and Technology of Synthetic Leather Sichuan University-Lishui University, Lishui 323000,*

Corresponding Authors:

Dr. Jun Yan; Email: yanjun2018@nun.edu.cn;

Prof. Zefeng Wang; Email: shangk72@163.com;

Prof. Shengwei Guo; Email: shengwei@nun.edu.cn;

Contents

Experimental Section

Materials.

All chemicals and reagents were of analytical grade and used as received without further purification. 1-(3,5-Difluorophenyl)-2,2,2-trifluoroethanone (97%) and 2,2,2-trifluoroacetophenone (98%) were purchased from Bide Pharmatech Co., Ltd. Anhydrous dimethylsulfoxide (DMSO), anhydrous N, N-dimethylformamide (DMF), and anhydrous tetrahydrofuran (THF) were purchased from J&K Chemical Co., Ltd. The monomer, 6,6'-(1,4-phenylene)bis(1,3,5-triazine-2,4-diamine), was synthesized following a previously reported literature procedure.[1]

Synthesis of PKANs.

Synthesis of PKAN-2. In a dried 50 mL Schlenk flask were placed 6,6'-(1, 4-phenylene)bis(1,3,5-triazine-2,4-diamine) (0.50 g, 1.6 mmol), 2, 2, 2-trifluoro-1-phenylethanone (0.59 g, 3.38 mmol), and anhydrous DMSO (30 mL). The mixture was stirred continuously at 170℃ for 72 h. After cooling to room temperature, the precipitate was collected by vacuum filtration and washed sequentially with DMSO, DMF, and THF (3 × 20 mL each). The product was further purified by Soxhlet extraction with THF for 48 h. The resulting solid was dried overnight under vacuum at 120℃ to afford PKAN-2 as a white solid in 58% yield.

Synthesis of PKAN-3. PKAN-3 was prepared following the procedure for PKAN-2, substituting 1-(3,5-difluorophenyl)-2,2,2-trifluoroethanone (0.73 g, 3.40 mmol) for 2,2,2-trifluoro-1-phenylethanone. The product was obtained as a white solid powder. Yield: 52%.

Material Characterization

Morphology was analyzed by field-emission scanning electron microscopy (FE-SEM; ZEISS SUPRA™ 55) and high resolution transmission electron microscopy (HR TEM; Thermo Fisher Scientific Talos F200x). Powder X-ray diffraction (PXRD) patterns were acquired on a Rigaku D Max 2400 diffractometer (Cu Kα radiation, 40 kV, 200 mA) at $2^{o}\cdot min^{-1}$. Thermogravimetric

analysis (TGA) was performed on a TA Instruments Q50 analyzer under N_2 (10 °C·min^{-1} to 800 °C). Chemical structure was assessed by Fourier transform infrared (FTIR) spectroscopy (ThermoFisher Scientific Nicolet™ 20XB) and solid-state ^{13}C CP/TOSS NMR spectroscopy (Bruker AVANCE III HD 600 MHz). Surface composition and bonding were determined by X-ray photoelectron spectroscopy (XPS; Al K_α source, 1486.6 eV), with binding energies referenced to C_{1s} at 284.80 eV. N_2 physisorption isotherms at 77 K were measured using a Quantachrome Autosorb iQ3 analyzer. Pure-component N_2 and SF_6 adsorption isotherms (273 K, 298 K) were obtained on a BSD-PMC analyzer (BeiShiDe Instrument). Ideal Adsorbed Solution Theory (IAST) selectivities for SF_6/N_2 (0.1:0.9 v/v) were calculated from single-component isotherm fits using the single-site Langmuir-Freundlich model. Separation performance was evaluated using a fixed-bed quartz column (ID 0.6 cm, length 7.5 cm) packed with activated PKANs (0.50 g; He flow, 40 mL min^{-1}, 373 K, 3 h). A 10% SF_6/90% N_2 (v/v) mixture was introduced at 5 mL·min^{-1}, 298 K. Effluent concentrations were monitored in situ by mass spectrometry (Pfeiffer Vacuum ThermoStar), tracking ion currents at m/z 89 (SF_3^+) and 28 (N_2^+) Adsorption capacities were derived from breakthrough curves.

Ideal Adsorbed Solution Theory (IAST) Selectivity

The pure component isotherms of SF_6 and N_2 were fitted with the single-site Langmuir (SSL) model.

$$N = \frac{A \times B \times P^c}{1 + B \times P^c} \quad \text{S1}$$

Where N is molar loading of adsorbate (mmol/g), P is pressure (kPa), A is saturation loading (mmol/g), B is a parameter in the pure component Langmuir isotherm (kPa^{-1}), C is the parameter of Langmuir-Freundlich.

Pure-component isotherm fitting parameters were then used for calculating Ideal Adsorbed Solution Theory (IAST)[1] binary-gas adsorption selectivities, S, defined as

$$S = \frac{q_1/q_2}{P_1/P_2} \quad \text{S2}$$

In the equation, q_1 and q_2 are the molar loadings in the adsorbed phase in equilibrium with the bulk gas phase with partial pressures p_1 and p_2.

Computational Details

The geometric structures of PKANs were fully optimized via density functional theory (DFT) calculations, as implemented in the DMol3 module of Materials Studio software. These optimizations utilized the Perdew-Burke-Ernzerhof (PBE) exchange-correlation functional within the generalized gradient approximation (GGA) framework, providing a robust description of the electronic structure and molecular geometry. To elucidate charge distribution patterns and identify prospective adsorption sites, molecular electrostatic potential (ESP) surfaces were generated by projecting the ESP onto the electron density isosurface of optimized fragments from PKANs. Molecular electrostatic potential (ESP) surfaces were mapped onto the electron density isosurfaces of the optimized fragments to visualize charge distribution and identify favorable binding sites.

Adsorption energies (ΔE_{ads}) for the guest molecules (SF_6 and N_2) on PKAN-2 and PKAN-3 were evaluated using the Forcite module in Materials Studio. Initial geometry optimizations of the isolated adsorbates and host polymer were conducted with the Universal Force Field (UFF). Subsequently, composite structures comprising the adsorbate and PKANs were assembled and further optimized under UFF constraints. The adsorption energy was then derived from single-point energy evaluations, also employing UFF, according to the formula:

$$\Delta E_{ads} = E_{complex} - (E_{host} + E_{guest}) \quad \text{S3}$$

Here, ΔE_{ads} denotes the adsorption energy, while $E_{complex}$, E_{guest} and E_{host} represent the total energies of the adsorbate-polymer complex, the isolated polymer, and the isolated gas molecule, respectively. This approach yields a quantitative measure of binding affinity, accounting for van

der Waals and electrostatic contributions in a computationally efficient manner.

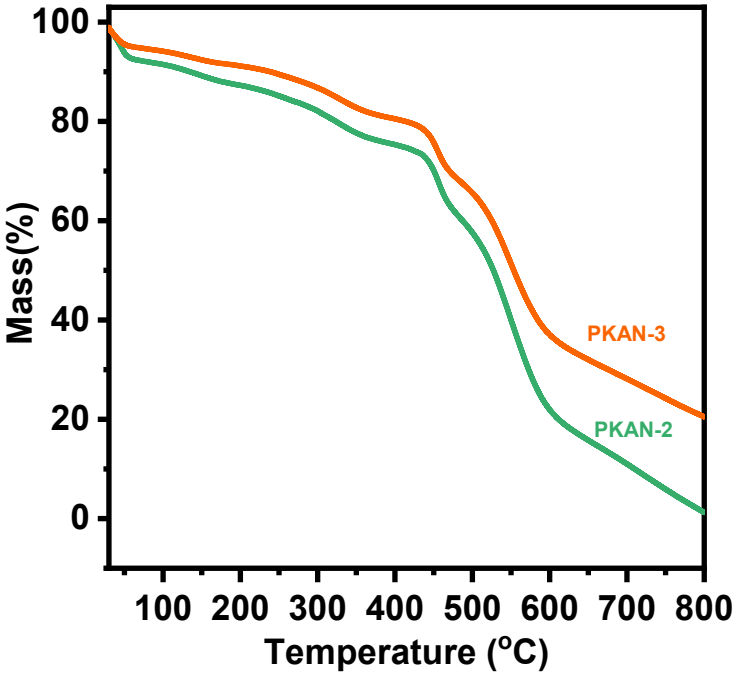

Figure S1. TGA curves of PKAN-2 and PKAN-3 under N_2 atmosphere.

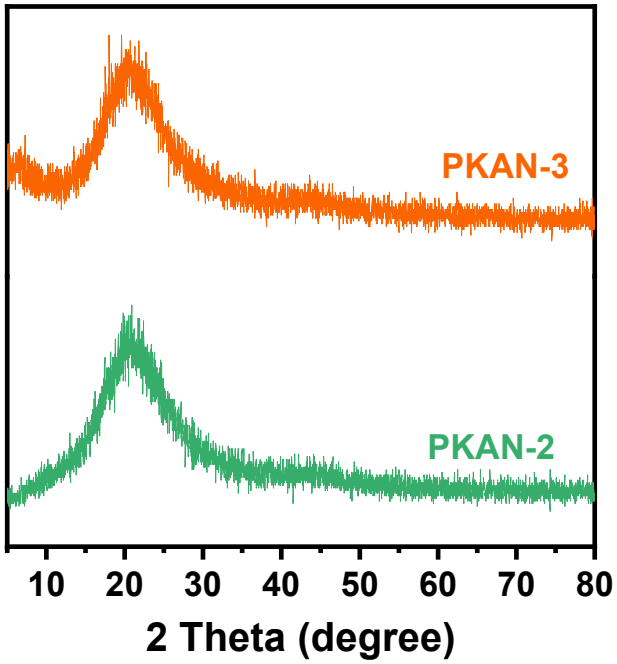

Figure S2. Powder X-ray diffraction (PXRD) patterns of PKAN-2 and PKAN-3.

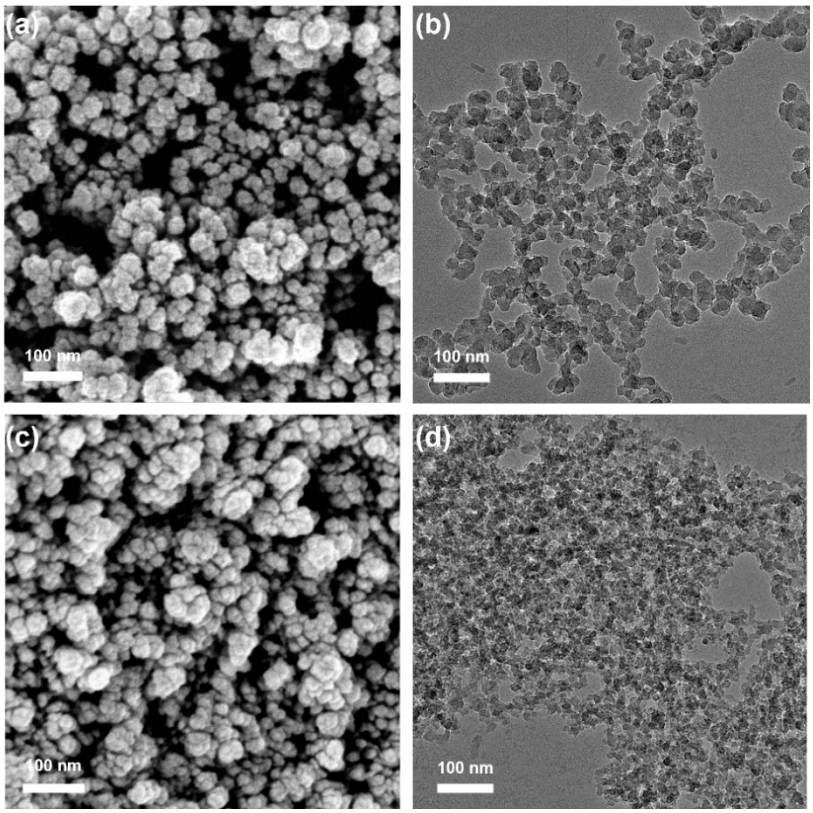

Figure S3. (a) FE-SEM image of PKAN-2; (b) HR-TEM image of PKAN-2; (c) FE-SEM image of PKAN-3; (d) HR-TEM image of PKAN-3.

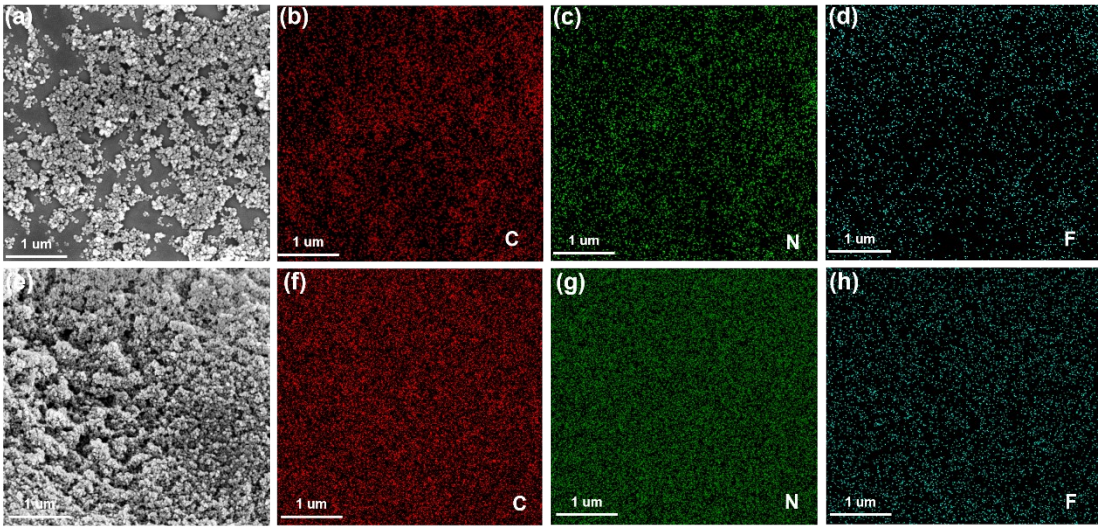

Figure S4. (a) SEM image of PKAN-2 and EDX elemental mapping images (b – d) for C, N, and F; (e) SEM image of PKAN-3 and EDX elemental mapping images (f – h) for C, N, and F.

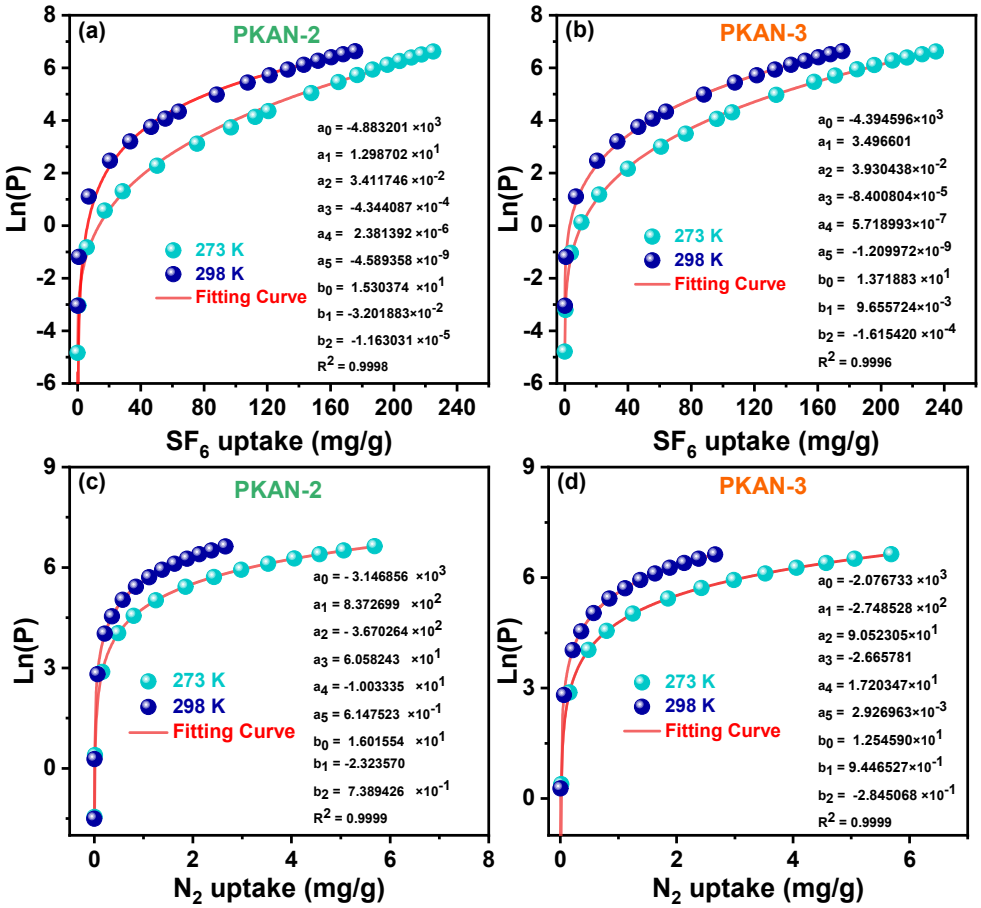

Figure S5. Virial equation fittings of (a) SF6 and (b) N_2 adsorption isotherms for PKAN-2 at 273 K and 298 K; (c) SF_6 and (d) N_2 adsorption isotherms for PKAN-3 at 273 K and 298 K.

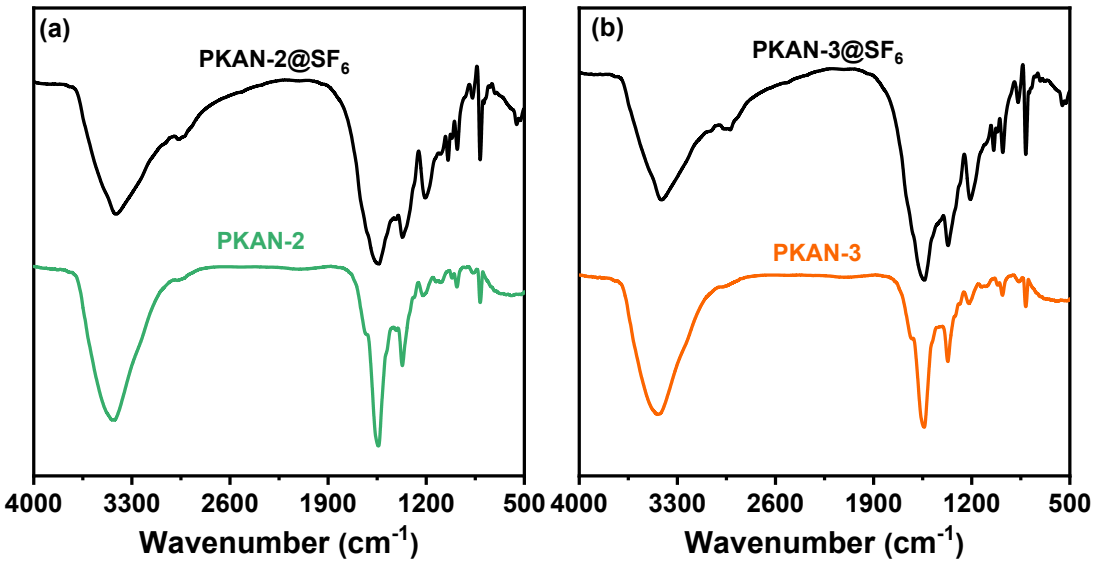

Figure S6. FTIR spectra of PKAN-2 and PKAN-3 before and after SF_6 adsorption.

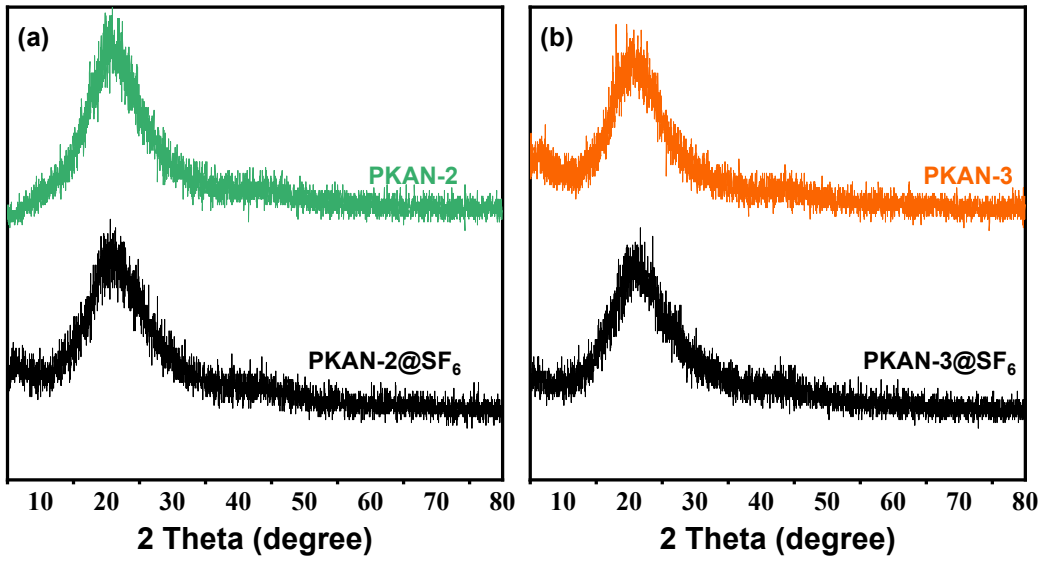

Figure S7. Powder X-ray diffraction (PXRD) patterns of PKAN-2 and PKAN-3 before and after SF_6 adsorption.

Table S1. Porosity parameters of PKAN-2 and PKAN-3.

Samples	S_{BET}（m^2/g）	S_{micro}（m^2/g）	V_{micro}（cm^3/g）	V_{total}（cm^3/g）	Pore size（nm）
PKAN-2	921	650	0.45	2.40	0.57, 1.06, 1.91
PKAN-3	864	432	0.40	2.41	0.52, 1.09, 3.93

Table S2. Single-Site Langmuir-Freundlich fitting parameters for SF_6 and N_2 adsorption on PKAN-2 and PKAN-3 at 298 K.

Sample	T/K	Gas	A(mmol/g)	B(kPa^{-C})	C	R^2
PKAN-2	**298 K**	**SF_6**	2.0383	6.9625×10^{-2}	0.6872	0.9997
		N_2	0.7396	1.3097×10^{-3}	1.0218	0.9999
PKAN-3	**298 K**	**SF_6**	2.6423	4.5075×10^{-2}	0.6299	0.9997
		N_2	0.6003	1.3519×10^{-3}	1.0693	0.9999

Table S3. SF_6 adsorption capacities, isosteric heats (Q_{st}), and N_2 selectivities for PKAN-2, PKAN-3, and reported porous organic polymers at 100 kPa and 298 K.

Materials	S_{BET} ($m^2 \cdot g^{-1}$)	SF_6 Uptake (mmol g^{-1})	Q_{st} (kJ • mol^{-1})	SF_6/N_2 selectivity	Ref
PKAN-2	921	1.28	40.5	150.1	This Work
PKAN-3	864	1.20	36.5	122.7	
PKAN-1	977	2.40	29.3	113	[2]
CPOF-12	1140	2.20	26.8	149.4	[3]
BrCOF-2	1602	1.38	20.6	~16.3	[4]
BrCOF-2-CF_3	1514	1.45	24.8	~38.6	[4]
POPTrA-4F	693.0	1.29	-	62.09 [a]	[5]
POPTrA-8F	507.1	1.12	-	27.08 [a]	[5]
PPy-POF	641.8	0.84	25.9	823.6	[6]
POPTrB-4F	775.5	-	30.25	62.88 [a]	[7]
POPTrB-8F	628.9	-	27.15	51.55 [a]	[7]
NMUCOF-1	991	1.11	26.6	37	[8]
CNOP-7	1270	1.90	30	73	[9]
TNOP-1	822	1.5	30	95	[10]
TNOP-2	605	0.92	26.6	77	[11]
TNOP-3	803	1.28	33.1	98	[11]
TNOP-4	891	1.62	33.5	105	[11]
TNOP-5	772	1.34	35.5	108	[11]
PAF-4F	1072.9	1.17	30.4	42.2 [a]	[12]
RCOF-1-	1139	3.46	27.0	83	[13]
RCOF-1-2	984	2.97	33.2	78	[13]
RCOF-1-3	945	2.49	27.7	88	[13]
RCOF-1-4	864	2.42	29.2	88	[13]

[a]SF_6/N_2=1:99; [b]IAST selectivity in 293 K; [c]IAST selectivity in 10 bar

References

1. J. Yan, J. Zhu, S. Tong, Q. Wang and Z. Wang, *ACS Appl. Mater. Interfaces*, 2024, **16**, 56181−56190.
2. Q. Wang, J. Zhu and J. Yan, *ACS Macro Lett.* , 2025, **14**, 1535−1542.
3. Y. Zhao, C. Meng, Y. Chen, W. Gong, G. Xing, D. Yuan and T. Ben, *Angew. Chem. Int. Ed.*, 2025, **64**, e202508493.
4. Q. Liao, C. Ke, X. Huang, D. Wang, Q. Han, Y. Zhang, Y. Zhang and K. Xi, *Angew. Chem. Int. Ed.*, 2021, **60**, 1411-1416.
5. W. Zhang, Y. Li, Y. Wu, Y. Fu, S. Chen, Z. Zhang, S. He, T. Yan and H. Ma, *Sep. Purif. Technol.*, 2022, **287**, 120561.
6. W. Zhang, Y. Li, Y. Wu, W. Huang, S. Wang, Y. Fu, W. Ma, X. Li and H. Ma, *ACS Appl. Mater. Interfaces* 2023, **15**, 29468-29477.
7. W. Zhang, Y. Wu, Y. Li, S. Chen, Y. Fu, Z. Zhang, T. Yan, S. Wang and H. Ma, *Macromolecules*, 2022, **55**, 1435-1444.
8. J. Zhu, Q. Wang, Z. Wang and J. Yan, *Acs Appl Polym Mater*, 2025, **7**, 9488-9495.
9. S. Tong, L. Yao, Q. Wang, J. Zhu, Z. Wang and J. Yan, *ACS Macro Lett.* , 2024, **13**, 1469-1475.
10. X. Yang, Q. Wang, J. Zhu, J. Yan and S. Guo, *ACS Materials Lett.* , 2025, **7**, 1940-1946.
11. J. Zhu, X. Chen, Q. Wang and J. Yan, *ACS Appl. Mater. Interfaces* 2025, **17**, 70029-70038.
12. W. Zhang, Y. Li, S. Wang, Y. Wu, S. Chen, Y. Fu, W. Ma, Z. Zhang and H. Ma, *ACS Appl. Mater. Interfaces* 2022, **14**, 35126-35137.
13. Q. Liao, H. Xu, C. Ke, Y. Zhang, Q. Han, Y. Zhang, Y. Xu, D. Wang and K. Xi, *Sep. Purif. Technol.*, 2023, **306**, 122595.